Noname manuscript No.
(will be inserted by the editor)

A direct scaling analysis for the sea level rise

Giuseppe Roberto Tomasicchio,
Letizia Lusito,
Felice D'Alessandro,
Ferdinando Frega,
Antonio Francone,
Samuele De Bartolo

Received: date / Accepted: date

Abstract The estimation of long-term sea level variability is of primary importance for a climate change assessment. Despite the value of the subject, no scientific consensus has yet been reached on the existing acceleration in observed values. The existence of this acceleration is crucial for coastal protection planning purposes. The absence of the acceleration would enhance the debate on the general validity of current future projections. Methodologically, the evaluation of the acceleration is a controversial and still open discussion, reported in a number of review articles, which illustrate the state-of-art in the field of sea level research.

In the present paper, the well-proven direct scaling analysis approach is proposed in order to describe the long-term sea level variability at 12 worldwide-selected tide gauge stations.

For each of the stations, it has been shown that the long-term sea level variability exhibits a trimodal scaling behaviour, which can be modelled by a power law with three different pairs of shape and scale parameters. Compared to alternative methods in literature, which take into account multiple corre-

---

G.R. Tomasicchio, L. Lusito, F. D'Alessandro, S. De Bartolo
Department of Engineering for Innovation,
University of Salento, Campus Ecotekne,
Via Monteroni, 73100 Lecce (LE), Italy
E-mail: roberto.tomasicchio@unisalento.it
E-mail: letizia.lusito@unisalento.it
E-mail: felice.dalessandro@unisalento.it
E-mail: samuele.debartolo@unisalento.it

F. Frega, A. Francone
Department of Civil Engineering,
University of Calabria,
Via P. Bucci, 87036 Arcavacata di Rende (CS), Italy
E-mail: ferdinando.frega@unical.it
E-mail: antonio.francone@unical.it

lated factors, this simple method allows to reduce the uncertainties on the sea level rise parameters estimation.

1 Introduction

One of the present-day challenges is how to use science to cope with problems that can arise from complex natural phenomena that are not yet completely understood. One such phenomenon is the long-term sea level variability. Sea level is considered a key indicator of climate change and its estimation provides an essential constraint for global climate models [1, 28] `ref.28 added`. Since the sea level variability affects the coastal areas, it is also an important factor to be considered to mitigate the consequences of natural disasters both at the global level and at local/regional scales, particularly in coastal regions where there are substantial aggregations of population and properties [46,58], and for strategic beach-management plans [8, 9, 20, 50]. Moreover, sea level variability is a key factor in compound flood hazard assessments since coastal cities that are vulnerable to this phenomenon are also at risk for flooding from other correlated drivers (e.g. extreme coastal high tide, storm surge, porous media and river flow) [7, 27, 30, 33, 41–45]. `ref.30 added`

In this context, long-term sea level time series recorded at coastal tide gauges are particularly valuable [17, 29, 37, 38, 55, 57]. `ref.17, 29 added` In literature, extensive studies have been devoted to exploring sea level variability. The Intergovernmental Panel on Climate Change (IPCC), an international organisation responsible for assessing the scientific basis of climate change, its impacts and future risks, warned that at current trends, the projected increments in mean sea level (MSL) for the year 2100, relative to the 1986–2005 period, $\overline{\Delta}_{s,\mathrm{IPCC}}$, are 400 mm, 470 mm, 480 mm or 630 mm, for the *Representative Concentration Pathways* scenarios indicated as *RCP2.6*, *RCP4.5*, *RCP6.0* and *RCP8.5*, respectively. However, from the tide gauge records, the acceleration required to reach these large projected MSL rises over the course of the 21$^{\mathrm{st}}$ century is not evident. Even though the measurement of this acceleration is a topic with a long standing history [6, 13, 26], the most recent debate was initiated by a series of publications [21–23] that raised concerns about the general validity of the sea level projections; the authors did not find any acceleration in the sea level in U.S.A. tide gauge records during the 20$^{\mathrm{th}}$ century. Instead, for each time period they considered, the records showed small decelerations that are consistent with a number of earlier studies of worldwide gauge records [14, 54, 56]. By using a different approach in data analysis, other researchers [12, 40] have found the arguments of [21–23] not convincing and showed that accelerations are present.

It is worth to point out that the uncertainties on the methodology and interpretation of the results are not only restricted to the USA tide gauge records. Different studies reported that tide gauge data around Australia do not show any sign of acceleration [2,21–23,53]. An opposite explanation is given by [24], who showed that the observed acceleration is in line with those proposed by [25]. These contradictory results underline the importance of properly quantifying the uncertainties associated to each method.

The authors in [51] tried to shed light on the controversial discussion of the quantification of the MSL rise by providing a comprehensive review of the trend methods used so far (for a total of 30 methods). The authors believe that much of the misunderstandings/controversies in the scientific community are due to the different mathematical or statistical characteristics of the considered models: a different approach may lead to contradictory acceleration-deceleration inferences. Similar conclusions have been reached in [49].

In the last decade, some approaches based on the scaling analysis for the characterisation (and quantification) of long-term sea level variability in space and time have been proposed [5, 11, 15, 16, 32, 34]. These approaches have not been included in the set of 30 methods reviewed in [51].

Following [1], a sea level variability process exhibits scale invariance if its spectral density function follows a power-law behaviour for frequencies approaching zero. This power-law-built approach is based on the definition of the scale parameter. The value of this parameter defines not only long memory but also other kinds of scaling behaviour, as for example, white noise, short range stationarity and random walk. Thus, the estimation of the scale parameter of a sea level tide gauge record provides an alternative and complementary way of characterising the low frequency structure of the sea level variability.

A further approach for the scaling analysis of sea level records has been proposed by [59]. This approach is based on a multi-fractal temporally weighted de-trended fluctuation analysis (MF-TWDFA). This can be considered an extension of the multi-fractal de-trended fluctuation analysis (MF-DFA), that is suitable to identify long-range correlation and multi-scaling behaviour of the MSL rise in Hong Kong.

To our knowledge, among the currently available scaling-based trend methods in literature, a procedure involving a direct scaling analysis (DSA) has not been yet applied in sea level research [10].

The focus of the present work is to examine the long-term variability of the observed annual MSL, indicated in the following as $\bar{h}$, at 12 selected tide gauge stations (TGS) with a direct scaling analysis.

The paper is organised as follows. Section 2 describes the tide gauge dataset used to retrieve the information related to $\bar{h}$ and the adopted DSA approach. Section 3 presents the application of the DSA method to 12 selected TGS. Section 4 shows how an estimate of the sea level variability can be obtained with the DSA approach. It also presents some preliminary projections for the selected TGS relative to the year 2100. Finally, Section 5 draws the conclusion of the paper, indicating lower values of MSL projections in comparison with the IPCC scenarios.

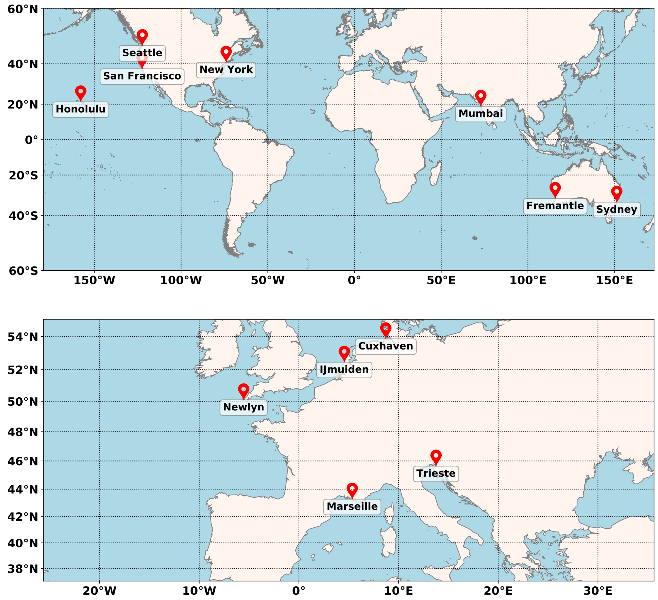

Fig. 1 Locations of the 12 selected TGS.

2 Data processing and methods

2.1 Tide Gauge Dataset and selected stations

In the present study, tide gauge data extracted from the database of the Permanent Service for Mean Sea Level (PSMSL) have been considered [19, 36]. The PSMSL is the global data bank of long-term sea level information, obtained from tide gauges. The PSMSL receives monthly and annual MSL values from almost 200 national authorities, distributed around the world, responsible for the sea monitoring in each country or region. In order to define time series of sea level records at each station, the monthly and annual means have to be reduced to a common datum. This reduction is performed by the PSMSL by making use of the tide gauge datum history provided by the supplying authority. This data set forms the so-called 'Revised Local Reference' (or 'RLR') dataset. In general, only RLR data should be used for time series analysis.

In this work, data sets of observed annual MSL time series from 12 selected TGS have been analysed. All of them have long and continuous records, covering at least 78 years, from 1916 to 1993, with gaps < 1 year. Figure 1 shows the 12 selected TGS, located in Northern Europe (Newlyn, UK; IJmuiden, The Netherlands; Cuxhaven, Germany), Southern Europe (Trieste, Italy and Marseille, France), United States of America (San Francisco, Seattle, New York, Honolulu), India (Mumbai), Australia (Fremantle and Sydney).

Table 1 summarises the characteristics of the 12 TGS, by including the geographic coordinates, the time of the available sea levels records and Y, the length in years of the data set.

Figure 2 shows the time series of $\bar{h}$ from the 12 selected TGS for the period 1916–1993 (the time interval that is common to all the data sets considered).

Table 1 Characteristics of the investigated TGS.

Country	**Location**	**PSMLS ID**	**Longitude**	**Latitude**	**Recording Time**	**N. years Y**
Germany	Cuxhaven	7	8°43'00"E	53°52'00"N	1843–2016	174
The Netherlands	IJmuiden	32	4°33'16"E	52°27'43"N	1872–2016	145
United Kingdom	Newlyn	202	5°32'34"W	50°06'10"N	1916–2016	101
France	Marseille	61	5°21'13"E	43°16'43"N	1885–2016	132
Italy	Trieste	154	13°45'30"E	45°38'50"N	1875–2016	142
USA	New York	12	74°00'47"W	40°42'00"N	1856–2016	161
USA	Seattle	127	122°20'17"W	47°36'06"N	1899–2016	118
USA	San Francisco	10	122°27'54"W	37°48'24"N	1855–2016	162
USA	Honolulu	155	157°52'00"W	21°18'24"N	1905–2016	112
India	Mumbai	43	72°49'59"E	18°55'00"N	1878–2010	133
Australia	Sydney	65	151°13'59"E	33°51'00"S	1886–1993	108
Australia	Fremantle	111	115°44'2"E	32°03'20"S	1897–2015	119

2.2 DSA approach

The scaling relationship of $\bar{h}$ has been examined following a DSA approach [18, 31, 47]. This approach has been used to provide information about a possible simple or multimodal behaviour of the observed annual MSL at the 12 selected TGS, for the period 1916 - 1993.

Specifically, for the considered TGS, the values of $\bar{h}$ have been rescaled to a common starting level ('0') by subtracting the data set minimum value, $\overline{h}_{min}$, from all the records:

$$\overline{\Delta} = \overline{h} - \overline{h}_{min} \tag{1}$$

The analysed variable then becomes the observed annual MSL increment, defined as $\overline{\Delta}$.

The cumulative mass function (cmf) of $\overline{\Delta}$, P($\overline{\Delta} \geq \overline{\Delta}_s$), with varying measure partition $d\overline{\Delta}$, fits well with a power law:

$$P(\overline{\Delta} \geq \overline{\Delta}_s) \sim a \cdot (\overline{\Delta}_s)^{-b} \tag{2}$$

where a and b are the shape and scale parameters, respectively, and $\overline{\Delta}_s$ is the threshold minimum value of the observed annual MSL increment observed in any class partition of the measure $\overline{\Delta}+d\overline{\Delta}$. This scaling law, in which the parameters a and b are invariant, can be determined by fitting straight lines to

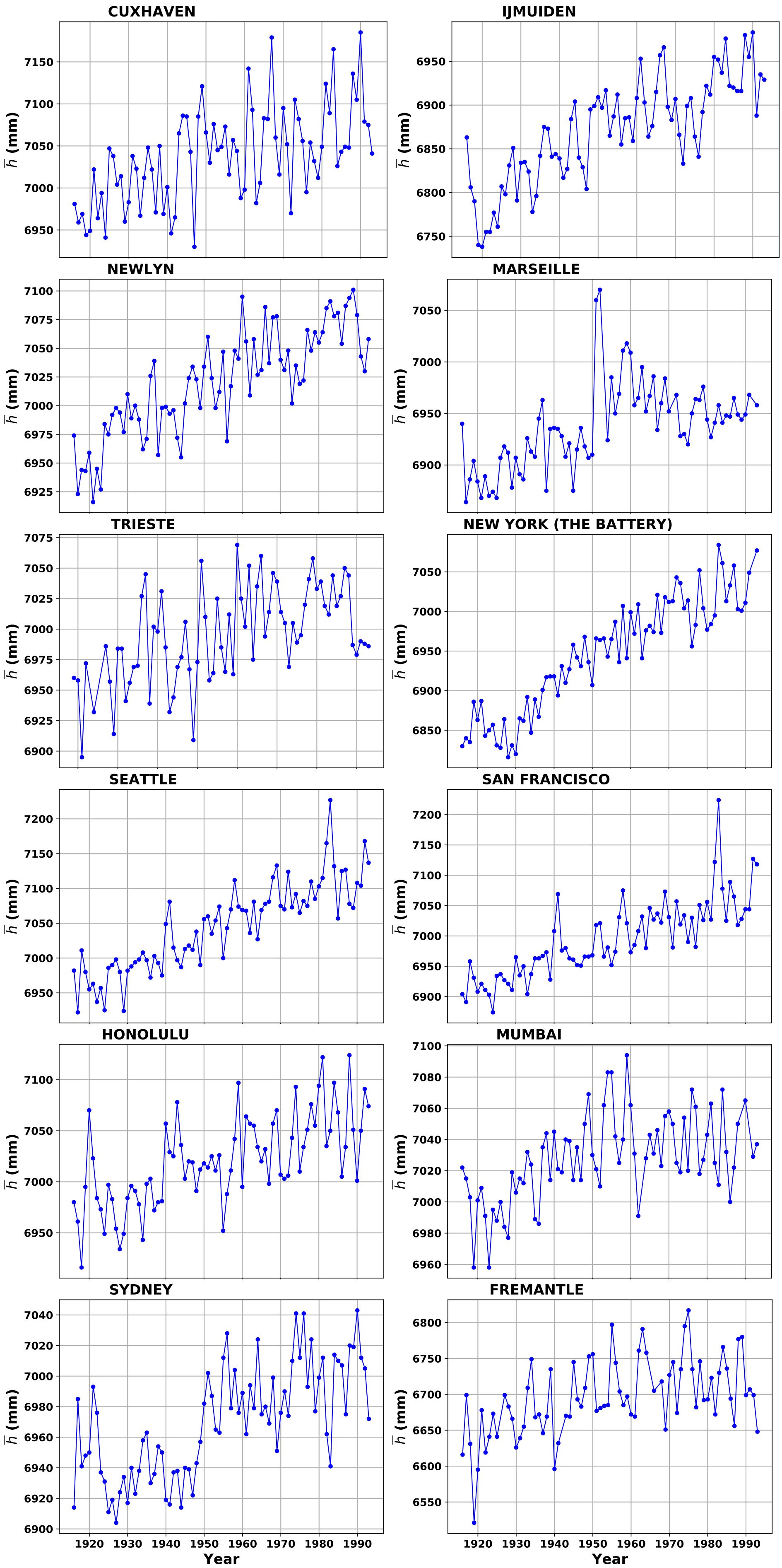

Fig. 2 Observed annual MSL for the period 1916–1993.

$\overline{\Delta}$ data sets for each spatial partition on log-log scale, namely, by the following relationship:

$$log[P(\overline{\Delta} \geq \overline{\Delta}_s)] \sim log(a) - b \cdot log(\overline{\Delta}_s) \tag{3}$$

In the present application, the fitting ranges have been determined as those resulting in the maximum determination coefficient, R^2, of the least squares linear regression [31]. This procedure allows the definition of the lower and upper values of the physical limits, $\overline{\Delta}_{s,inf}$ and $\overline{\Delta}_{s,sup}$ which could even not be coincident with the minimum or maximum values of $\overline{\Delta}$, therefore the scaling range is defined between these limits. This range can have a simple or multi-scaling behaviour. The latter aspect would be highlighted by the presence of multiple consecutive scaling regimes with different slopes. In particular, in the present work, (see Sect. 3.1) such behaviour appears to be characterised by the presence of three scaling regimes, showing a multimodal nature.

3 Results

The observed annual MSL increment time series from 12 selected TGS have been analysed following the DSA approach based on Eqs. 2 and 3. In the following, the TGS in San Francisco has been selected as representative case. The fitting procedure for Eq. 3 has been carried out with a numerical algorithm based on the libraries Scipy [35] and Numpy [52] of Python 2.7 [39].

3.1 Scaling analysis

Figure 3 shows the relationship between log[P($\overline{\Delta} \geq \overline{\Delta}_s$)] and log($\overline{\Delta}_s$). A value of 1 mm has been considered for $d\overline{\Delta}$, corresponding to the maximum resolution of the measure. The black line represents the cmf of $\overline{\Delta}_s$. It can be observed that the cmf exhibits three scaling regimes, indicated as 1, 2 and 3. The red dashed line depicts the piecewise linear fitting function.

The DSA method, through the fitting procedure based on Eq. 3, allows to determine the values of the scaling range limits, $\overline{\Delta}_{s,inf}$ and $\overline{\Delta}_{s,sup}$. From these, the corresponding limits of the observed annual MSL, defined as $\overline{h}_{inf}$ and $\overline{h}_{sup}$, can be determined:

$$\overline{h}_{inf} = \overline{\Delta}_{s,inf} + \overline{h}_{min} \tag{4}$$

$$\overline{h}_{sup} = \overline{\Delta}_{s,sup} + \overline{h}_{min} \tag{5}$$

Moreover, the method allows to determine their corresponding probabilities, $P(\overline{h}_{inf})$ and $P(\overline{h}_{sup})$, and the differences $\overline{h}_{sup} - \overline{h}_{inf}$ and $P(\overline{h}_{inf}) - P(\overline{h}_{sup})$. All these observations are very important to quantify the behaviour of the sea level variability in each of the considered locations.

Table 2 summarises the results of the DSA analysis for the 1^{st}, 2^{nd}, and 3^{rd} scaling regimes at each of the selected TGS.

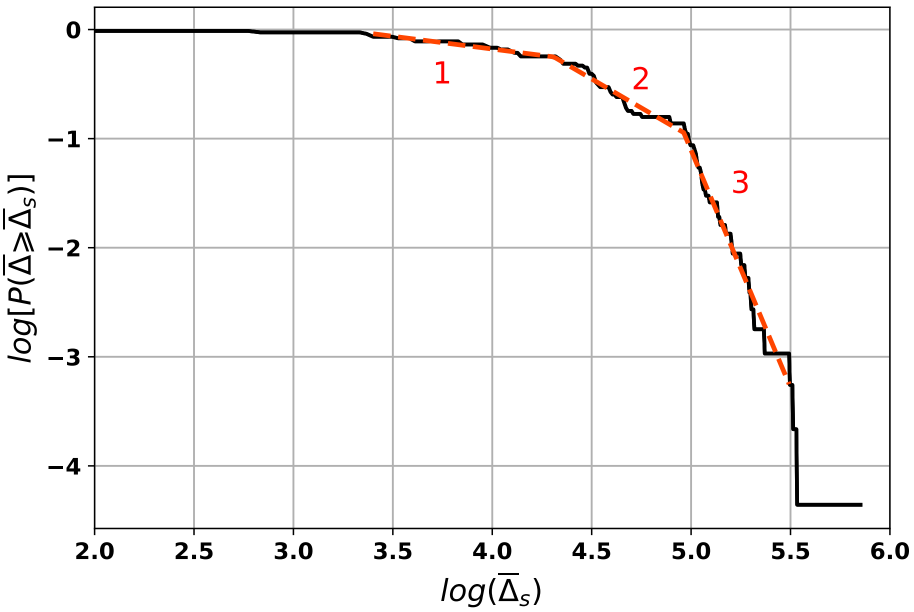

Fig. 3 Observed trimodal scaling behaviour at San Francisco TGS, for the period 1916 - 1993.

The largest differences between $\overline{h}_{sup}$ and $\overline{h}_{inf}$ are observed in New York (99 mm), Seattle (89 mm) and San Francisco (100 mm) for the 1^{st}, 2^{nd} and 3^{rd} scaling regimes, respectively. The smallest differences between $\overline{h}_{sup}$ and $\overline{h}_{inf}$ are observed in Mumbai (31 mm and 34 mm) for the 1^{st} and 2^{nd} scaling regimes and in Newlyn (14 mm) for the 3^{rd} scaling regime.

To evaluate the existence of a spatial homogeneous scaling behaviour among the considered TGS, the values of the scale parameter b have been analysed. Although similar values of b have been observed for the 1^{st}, 2^{nd} and 3^{rd} scaling regimes (e.g. Seattle, Honolulu, San Francisco), a certain non-uniformity, showing a multi-scaling behaviour, already highlighted in other works on similar subjects [59], has been found. Specifically, the variability of the b exponent, between 0.05 $\pm$ 0.01 and 0.53 $\pm$ 0.02 for the 1^{st} regime, 0.84 $\pm$ 0.03 and 3.31 $\pm$ 0.07 for the 2^{nd} regime, 3.58 $\pm$ 0.07 and 13.09 $\pm$ 0.95 for the 3^{rd} regime, suggests that a geographical correlation is not clearly evident.

3.2 Scaling regimes variation in time

The DSA approach has been applied to investigate the temporal variations of the observed annual MSL increment. In this case, the available entire data set has been considered in the analysis (Table 1), partitioned in other two data sets: the first, PTS1, spans 50 years (covering the period 1855–1905) and the second, PTS2, spans 100 years (for the period 1855–1955). The entire data

Table 2 DSA results for the 1^{st}, 2^{nd}, and 3^{rd} scaling regimes at the selected TGS ($d\overline{\Delta} = 1$ mm), for the period 1916 - 1993.

Regime	$\bar{h}_{inf}$ [mm]	$\bar{h}_{sup}$ [mm]	$P(\bar{h}_{inf})$	$P(\bar{h}_{sup})$	$\bar{h}_{sup}-\bar{h}_{inf}$ [mm]	$P(\bar{h}_{inf})-P(\bar{h}_{sup})$	b	$log(a)$
SAN FRANCISCO: $\bar{h}_{min}$ = 6874 mm, R^2 = 0.993								
1^{st}	6904	6948	0.962	0.778	44	0.184	0.23	0.76
2^{nd}	6948	7016	0.778	0.389	68	0.389	1.06	4.33
3^{rd}	7016	7116	0.389	0.039	100	0.428	4.35	20.64
SEATTLE: $\bar{h}_{min}$ = 6922 mm, R^2 = 0.987								
1^{st}	6937	6975	0.967	0.905	38	0.062	0.05	0.11
2^{nd}	6975	7064	0.905	0.469	89	0.436	0.67	2.56
3^{rd}	7064	7135	0.469	0.073	71	0.541	4.62	22.17
NEW YORK (THE BATTERY): $\bar{h}_{min}$ = 6816 mm, R^2 = 0.994								
1^{st}	6829	6928	1.000	0.667	99	0.349	0.20	0.55
2^{nd}	6928	6993	0.667	0.322	65	0.344	1.59	7.12
3^{rd}	6993	7056	0.322	0.054	63	0.376	5.88	29.34
NEWLYN: $\bar{h}_{min}$ = 6916 mm, R^2 = 0.992								
1^{st}	6943	7019	1.0000	0.602	76	0.472	0.43	1.49
2^{nd}	7019	7076	0.602	0.144	57	0.458	3.31	14.84
3^{rd}	7076	7090	0.144	0.048	14	0.192	13.09	64.51
CUXHAVEN: $\bar{h}_{min}$ = 6930 mm, R^2 = 0.994								
1^{st}	6945	7001	1.000	0.745	56	0.264	0.20	0.57
2^{nd}	7001	7046	0.745	0.491	45	0.254	0.86	3.39
3^{rd}	7046	7141	0.491	0.053	95	0.544	3.76	17.19
IJMUIDEN: $\bar{h}_{min}$ = 6738 mm, R^2 = 0.990								
1^{st}	6755	6825	0.997	0.819	70	0.177	0.12	0.33
2^{nd}	6825	6894	0.819	0.436	69	0.383	1.09	4.69
3^{rd}	6894	6965	0.436	0.058	71	0.494	5.43	26.59
TRIESTE: $\bar{h}_{min}$ = 6895 mm, R^2 = 0.993								
1^{st}	6932	6978	1.0000	0.706	46	0.303	0.44	1.59
2^{nd}	6978	7032	0.706	0.230	54	0.476	2.26	9.66
3^{rd}	7032	7054	0.230	0.053	22	0.283	9.86	47.01
MARSEILLE: $\bar{h}_{min}$ = 6864 mm, R^2 = 0.995								
1^{st}	6870	6906	0.968	0.811	36	0.158	0.09	0.13
2^{nd}	6906	6941	0.811	0.487	35	0.324	0.84	2.92
3^{rd}	6941	7010	0.487	0.051	69	0.539	3.58	14.86
SYDNEY: $\bar{h}_{min}$ = 6904 mm, R^2 = 0.994								
1^{st}	6914	6962	1.0000	0.609	48	0.452	0.31	0.78
2^{nd}	6962	7004	0.609	0.230	42	0.380	1.81	6.88
3^{rd}	7004	7026	0.230	0.051	22	0.280	7.60	33.59
FREMANTLE: $\bar{h}_{min}$ = 6521 mm, R^2 = 0.997								
1^{st}	6616	6665	0.970	0.776	49	0.193	0.53	2.40
2^{nd}	6665	6733	0.776	0.253	68	0.523	2.87	14.01
3^{rd}	6733	6790	0.253	0.048	57	0.301	7.13	36.83
HONOLULU: $\bar{h}_{min}$ = 6916 mm, R^2 = 0.995								
1^{st}	6949	6993	0.973	0.782	44	0.191	0.26	0.86
2^{nd}	6993	7047	0.782	0.293	54	0.490	1.86	7.83
3^{rd}	7047	7096	0.293	0.062	49	0.354	4.99	23.12
MUMBAI: $\bar{h}_{min}$ = 6958 mm, R^2 = 0.995								
1^{st}	6984	7015	0.973	0.741	31	0.232	0.34	1.08
2^{nd}	7015	7049	0.741	0.226	34	0.515	2.58	10.15
3^{rd}	7049	7071	0.226	0.066	22	0.292	5.89	25.12

set, PTS3, spans 162 years (1855–2016). Figure 4 shows the cmf for PTS1, PTS2 and PTS3. The black dashed lines depict the piecewise linear fits from the DSA analysis.

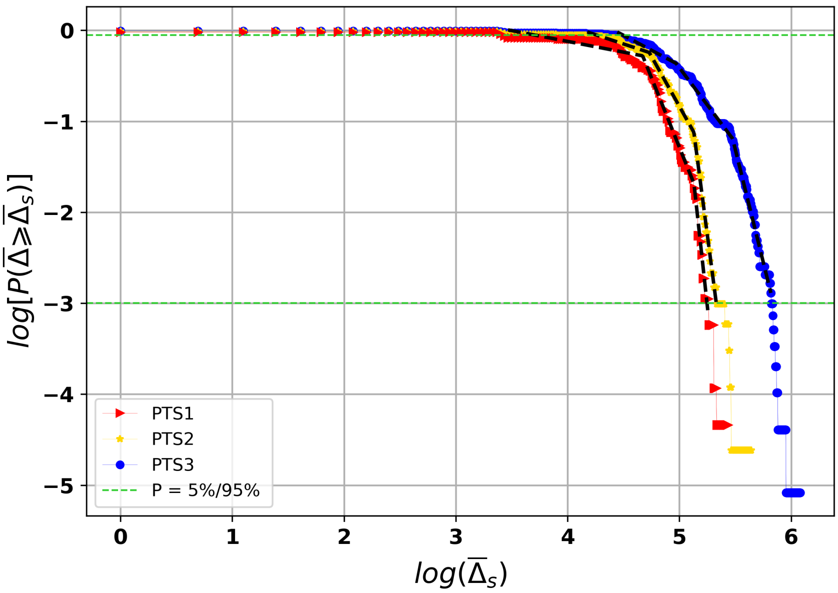

Fig. 4 DSA multi-scaling behaviour observed at the San Francisco TGS for the different data sets.

For each of the PTS data set, the DSA analysis has been applied excluding the following observed annual MSL increments that define the physical cut-offs of the cmfs:

$$\overline{\Delta}_s < \overline{\Delta}_{s,min} \text{ with } P(\overline{\Delta}_s \geq \overline{\Delta}_{s,min}) = 95\% \tag{6}$$

$$\overline{\Delta}_s > \overline{\Delta}_{s,max} \text{ with } P(\overline{\Delta}_s \geq \overline{\Delta}_{s,max}) = 5\% \tag{7}$$

As summarised in Table 3, the scale parameter, b, shows a different behaviour in time, thus highlighting a sea level variability. In particular, with reference to the 1^{st} scaling regime, the scale parameter b increases ($\overline{\Delta}_s$ interval decreases) with the length of the time period. On the contrary, for the scaling regimes 2^{nd} and 3^{rd}, b decreases ($\overline{\Delta}_s$ interval increases).

Specifically, with reference to the 3^{rd} scaling regime, the lowest value of b (cmf mildest slope) has been obtained in PTS3, which corresponds to larger intervals of observed $\overline{\Delta}_s$.

Table 3 DSA scale parameter observed at San Francisco TGS.

Data set	Number of years	Regime	b
		1^{st}	0.24
PTS1: 1855–1905 years	50	2^{nd}	3.06
		3^{rd}	11.27
		1^{st}	0.41
PTS2: 1855–1955 years	100	2^{nd}	2.20
		3^{rd}	9.37
		1^{st}	0.65
PTS3: 1855–2016 years	162	2^{nd}	1.64
		3^{rd}	4.96

4 Sea level future projections

In order to obtain information about future projections of annual MSL, the DSA analysis for each of the 12 selected TGS has been conducted for the entire data set and for partial data sets 25, 50, 75, 100, 125 and 150 years long, counted from the first observation; as a consequence, the number of partial data sets, N, is equal to Y/25 (Table 4).

Table 4 Recording time Y and number of partial data sets N for the investigated TGS.

TGS	Y	N
San Francisco	162	6
Seattle	118	4
New York	161	6
Honolulu	112	4
Newlyn	101	4
Cuxhaven	174	6
IJmuiden	145	5
Trieste	142	5
Marseille	132	5
Sydney	108	4
Fremantle	119	4
Mumbai	133	5

The total number of examined data sets is $N_{TS} = N{+}1$. As representative case, Figure 5 shows the results obtained for the San Francisco TGS. A total of 7 data sets has been considered: the 6 partial data sets and the available entire data set.

In order to obtain information about the extreme values of the observed $\overline{\Delta}_s$ and their probability of occurrence, the 3^{rd} scaling regime has been investigated, because it is used to model the lower range of probabilities (see Table 2). Since it describes the less frequent events, it is also a more direct representation of the amount of sea level fluctuations. On the contrary, the increments represented by the scaling regimes I and II, are directly connected to the secular growth which shows higher probability of occurrence. Within

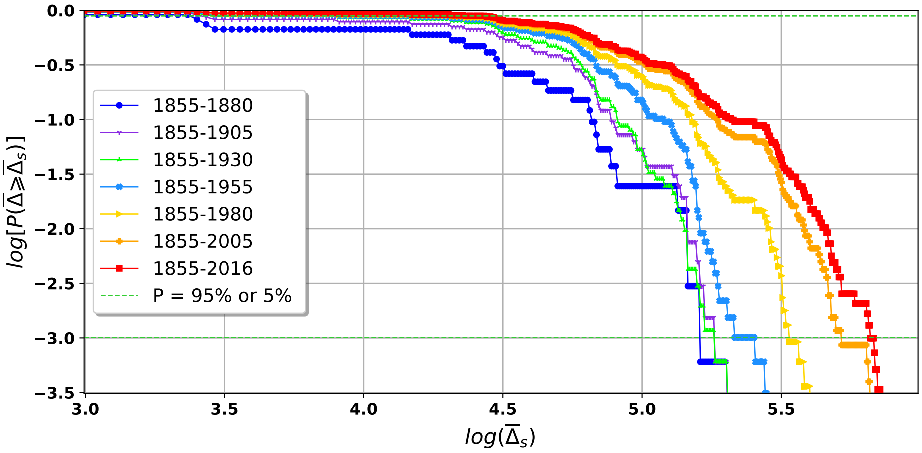

Fig. 5 DSA analysis for the San Francisco TGS (selected as representative).

the 3^{rd} scaling regime, for each considered data set, the largest values of observed $\overline{\Delta}_s$ corresponding to cmf $> 5\%$ (indicated with a dashed green line in Figure 5) have been selected. As an example, the largest observed $\overline{\Delta}_s$ in the data set 1855-1880 is 182 mm, with cmf $= 8\%$.

The cmfs relative to each data set, depicted with different colours in Figure 5, showed a different behaviour in time. In particular, kept constant a value of $\overline{\Delta}_s$, the cmf increases with the length of the data set. With reference to the data set 1855–1905, the observed $\overline{\Delta}_s = 182$ mm showed a higher probability of occurrence (cmf $\approx 12\%$) compared to the data set 1855–1880. The different behaviour of the cmfs during the time indicates that the observed $\overline{\Delta}_s$ values increased, reaching the largest values in the data set 1855–2006 (red line).

Table 5 summarises the values of the largest observed $\overline{\Delta}_s$ in the 3^{rd} scaling regime at the San Francisco TGS for the different data sets.

Table 5 Largest observed $\overline{\Delta}_s$ in different data sets at the San Francisco TGS.

Data set	Number of years	$\overline{\Delta}_s$ [mm]
1855–1880	25	182
1855–1905	50	192
1855–1930	75	192
1855–1955	100	206
1855–1980	125	251
1855–2005	150	303
1855–2016	162	336

In order to have a comparison with the IPCC projections, for each TGS, the observed annual MSL values ($\overline{h}$) in the years 1986–2005, have been considered, and, with reference to this time interval, the means of these values ($\overline{h}_\mu$) have

Table 6 Sea level projections for the year 2100 for each TGS: determination coefficient R^2 and the estimated projected $\overline{\varDelta}_s$ and $\overline{h}$.

TGS	R^2	**2100** $\overline{\varDelta}_s$ **[mm]**	**2100** $\overline{h}$ **[mm]**
San Francisco	0.992	642	7427
Seattle	0.981	431	7353
New York	0.995	691	7365
Honolulu	0.992	355	7212
Newlyn	0.985	359	7275
Cuxhaven	0.974	564	7306
IJmuiden	0.976	669	7344
Trieste	0.947	318	7125
Marseille	0.858	322	7145
Sydney	0.915	160	7064
Fremantle	0.967	455	6976
Mumbai	0.975	214	7151

been calculated. For each $\overline{h}_\mu$, the IPCC *RCP* [25] scenario predictions for the year 2100, $\overline{\varDelta}_{s,IPCC}$, have been added; the resulting values are indicated as $\overline{h}_*$, namely:

$$\overline{h}_* = \overline{\varDelta}_{s,IPCC} + \overline{h}_\mu \tag{8}$$

From Eq. 8, it is possible to extract the IPCC increment, $\overline{\varDelta}_p$, with respect to the $\overline{h}_{min}$, as in the following:

$$\overline{\varDelta}_p = \overline{h}_* - \overline{h}_{min} \tag{9}$$

The values of the largest observed $\overline{\varDelta}_s$ and the values of $\overline{\varDelta}_p$ are shown in Figure 6 for each of the selected TGS. A fitting procedure, based on the least-square minimisation method, has been applied to the largest observed $\overline{\varDelta}_s$ values, represented as blue dashed line. An extrapolation of the fitting function (blue dotted line) allows to give an estimation of the observed annual MSL increase up to the year 2100. A 95% confidence level band has been considered. The fitting procedure outlined two different behaviours for the selected TGS. In particular, San Francisco and IJmuiden, showed a second-degree polynomial law, whereas the others follow a linear trend.

For each considered TGS, lower values of $\overline{\varDelta}_s$ compared with the projections for the year 2100 from all the IPCC scenarios have been obtained [25]. For the IJmuiden and San Francisco TGS, characterised by a non-linear fitting function, values of projected $\overline{\varDelta}_s$ result in agreement with IPCC scenarios *RCP2.6* and *RCP4.5* [25].

Table 6 summarises, for each TGS, the determination coefficient R^2 and the estimated projected $\overline{\varDelta}_s$ and $\overline{h}$.

5 Conclusions

A methodology, based on a direct scaling analysis (DSA) of long and continuous records of mean sea level (MSL), covering at least 78 years from 1916

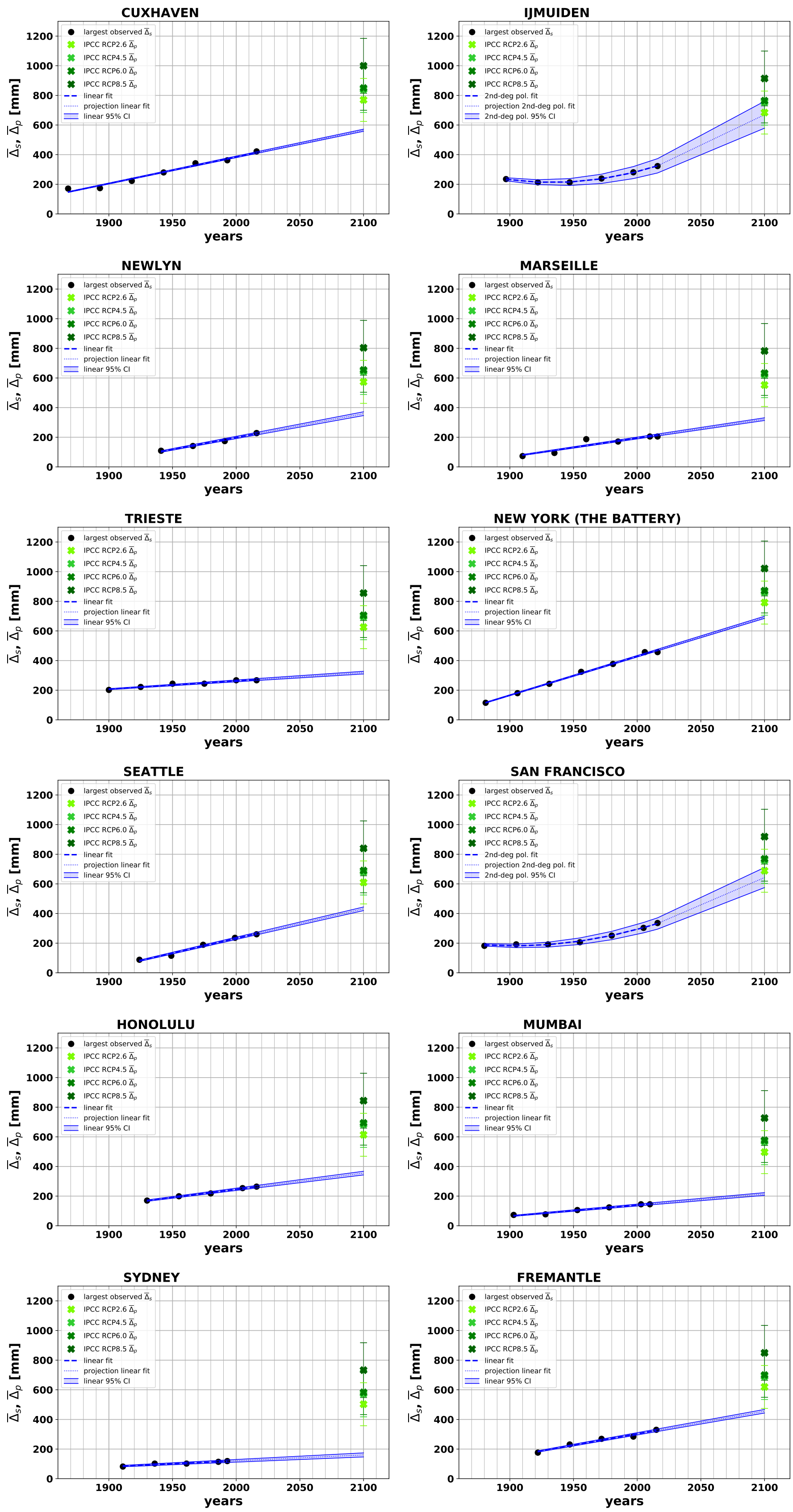

Fig. 6 Projected observed annual MSL increments for the 12 selected TGS. The projections calculated according to the IPCC scenarios are also shown.

to 1993, at 12 selected tide gauge stations, has been applied. The approach allowed to get insights about the scale invariance of the parameters characterising the cumulative mass functions (cmf) and the local predictions of the sea level variability. The cumulative mass function can be modelled with a piecewise power law function. Specifically, this function is characterised by the presence of three scaling regimes, showing a multi-scaling nature of the cmf behaviour. Following this approach, for the three observed scaling regimes, the minimum and maximum limits and the scale parameters have been estimated. In general, except few cases among those considered, the scale parameters do not exhibit correlation and spatial invariance, indicating a multiscaling behaviour on a geographical basis. This result is in agreement with already published results [59]. The overall analysis, further to highlight multi-scaling features, shows the possibility of adopting the same piecewise approach to predict the future sea level behaviour. For each considered TGS, lower values of $\overline{\Delta}_s$, relative to the projections for the year 2100 from all the IPCC scenarios, have been found with the possible exception of the two sites IJmuiden and San Francisco, characterised by a non-linear fitting function, in which the values of $\overline{\Delta}_s$ are only slightly lower compared to IPCC scenarios RCP2.6 and RCP4.5 [25]. These results would imply that considerable acceleration must take place in the following decades if the IPCC predictions are going to materialize. In a future work, a further analysis will be performed by separating the secular growth, which is visible in Figure 2, from the fluctuating behaviour of the data. A good assessment of the secular growth levels is of fundamental importance for the forecasting of the sea level variability in the future and the present fitting procedure could be improved through the use of different techniques. An alternative technique, to separate the secular growth from the fluctuations, would be the use of the 'Empirical Mode Decomposition' (EMD) method [3, 4, 48], which allows a clear separation of the different frequencies present in a signal and an eventual secular growth.

Acknowledgements This work was funded by the Apulia Region through the Regional Cluster Projects 'Start' and 'Eco-Smart Breakwater'. Moreover, the authors thank Prof. G. Salvadori for the fruitful discussions.

References

1. Barbosa, S.M., Silva, M.E., Fernandes, M.J.: Time Series Analysis of Sea-Level Records: Characterising Long-Term Variability. In: Donner R.V., Barbosa S.M. (eds) Nonlinear Time Series Analysis in the Geosciences. Lecture Notes in Earth Sciences **112** (2008). DOI 10.1007/978-3-540-78938-3_8
2. Boretti, A.: Is there any support in the long term tide gauge data to the claims that parts of Sydney will be swamped by rising sea levels? Coastal Engineering **64**(Supplement C), 161–167 (2012). DOI https://doi.org/10.1016/j.coastaleng.2012.01.006
3. Breaker, L., Ruzmaikin, A.: Estimating Rates of Acceleration Based on the 157-Year Record of Sea Level from San Francisco, California, U.S.A., vol. 29 (2013). DOI 10.2307/23353569
4. Chen, X., Feng, Y., Huang, N.E.: Global sea level trend during 1993–2012. Global and Planetary Change **112**, 26–32 (2014)

5. Chu, P.C., Lu, S., Chen, Y.: Temporal and spatial variabilities of the South China Sea surface temperature anomaly. Journal of Geophysical Research: Oceans **102**(C9), 20,937–20,955 (1997). DOI 10.1029/97JC00982
6. Church, J.A., White, N.J.: A 20^{th} century acceleration in global sea-level rise. Geophysical Research Letters **33**(1) (2006). DOI 10.1029/2005GL024826. URL http://dx.doi.org/10.1029/2005GL024826
7. Comegna, A., Coppola, A., Comegna, V., Severino, G., Sommella, A., Vitale, C.: State-space approach to evaluate spatial variability of field measured soil water status along a line transect in a volcanic-vesuvian soil. Hydrology and Earth System Sciences **14**, 2455 – 2463 (2010)
8. D'Alessandro, F., Tomasicchio, G.R.: Wave–dune interaction and beach resilience in large-scale physical model tests. Coastal Engineering **116**, 15–25 (2016). DOI https://doi.org/10.1016/j.coastaleng.2016.06.002
9. D'Alessandro, F., Tomasicchio, G.R., Musci, F., Ricca, A.: Dune erosion physical, analytical and numerical modelling. Coastal Engineering Proceedings (2012)
10. De Bartolo, S., Fallico, C., Ferrari, E.: Simple scaling analysis of active channel patterns in fiumara environment. Geomorphology **232**(Supplement C), 94–102 (2015). DOI https://doi.org/10.1016/j.geomorph.2015.01.001
11. Ding, X., Zheng, D., Chen, Y., Chao, J., Li, Z.: Sea level change in Hong Kong from tide gauge measurements of 1954–1999. Journal of Geodesy **74**(10), 683–689 (2001). DOI 10.1007/s001900000128
12. Donoghue, J.F., Parkinson, R.W.: Discussion of: Houston, J.R. and Dean, R.G., 2011. Sea-Level Acceleration Based on U.S. Tide Gauges and Extensions of Previous Global-Gauge Analyses. Journal of Coastal Research, 27(3), 409–417. Journal of Coastal Research **27**(5), 994–996 (2011). DOI 10.2112/JCOASTRES-D-11-00098.1
13. Douglas, B.C.: Global sea level rise. Journal of Geophysical Research: Oceans **96**(C4), 6981–6992 (1991). DOI 10.1029/91JC00064
14. Douglas, B.C.: Global sea level acceleration. Journal of Geophysical Research: Oceans **97**(C8), 12,699–12,706 (1992). DOI 10.1029/92JC01133
15. Douglas, B.C.: Global sea rise: A redetermination. Surveys in Geophysics **18**(2), 279–292 (1997). DOI 10.1023/A:1006544227856
16. Douglas, B.C., Kearney, M.T., Leatherman, S.P. (eds.): Sea Level Change in the Era of Recording Tide Gauge, chap. 3: Sea Level Rise: History and Consequences, pp. 37–64. Academic Press (2001). DOI https://doi.org/10.1016/S0074-6142(01)80006-1
17. Fawcett, L., Walshaw, D.: Sea-surge and wind speed extremes: optimal estimation strategies for planners and engineers. Stochastic Environmental Research and Risk Assessment **30**(2), 463–480 (2016). DOI 10.1007/s00477-015-1132-3. URL https://doi.org/10.1007/s00477-015-1132-3
18. Hergarten, S.: Self-Organized Criticality in Earth Systems. Springer-Verlag Berlin Heidelberg (2002)
19. Holgate, S.J., Matthews, A., Woodworth, P.L., Rickards, L.J., Tamisiea, M.E., Bradshaw, E., Foden, P.R., Gordon, K.M., Jevrejeva, S., Pugh, J.: New Data Systems and Products at the Permanent Service for Mean Sea Level. Journal of Coastal Research **29**(3), 493 – 504 (2013)
20. Houston, J.R.: Shoreline change in response to sea-level rise on florida's west coast. Journal of Coastal Research pp. 1243–1260 (2017). DOI 10.2112/JCOASTRES-D-17-00024.1
21. Houston, J.R., Dean, R.G.: Reply to: Donoghue, J.F. and Parkinson, R.W., 2011. Discussion of: Houston, J.R. and Dean, R.G., 2011. Sea-Level Acceleration Based on U.S. Tide Gauges and Extensions of Previous Global-Gauge Analyses. Journal of Coastal Research, 27(3), 409–417. Journal of Coastal Research pp. 997–998 (2011). DOI 10.2112/11A-00010.1
22. Houston, J.R., Dean, R.G.: Reply to: Rahmstorf, S. and Vermeer, M., 2011. Discussion of: Houston, J.R. and Dean, R.G., 2011. Sea-Level Acceleration Based on U.S. Tide Gauges and Extensions of Previous Global-Gauge Analyses. Journal of Coastal Research, 27(3), 409–417. Journal of Coastal Research pp. 788–790 (2011). DOI 10.2112/JCOASTRES-D-11A-00008.1

23. Houston, J.R., Dean, R.G.: Sea-Level Acceleration Based on U.S. Tide Gauges and Extensions of Previous Global-Gauge Analyses. Journal of Coastal Research pp. 409–417 (2011). DOI 10.2112/JCOASTRES-D-10-00157.1
24. Hunter, J.R., Brown, M.: Discussion of Boretti, A., 'Is there any support in the long term tide gauge data to the claims that parts of Sydney will be swamped by rising sea levels?', Coastal Engineering, 64, 161-167, June 2012. Coastal Engineering **75**, 1 – 3 (2013)
25. IPCC: Climate Change 2014: Synthesis Report. Contribution of Working Groups "I", "II" and "III" to the Fifth Assessment Report of the Intergovernmental Panel on Climate Change "[Core Writing Team, R.K. Pachauri and L.A. Meyer (eds.)]". IPCC, Geneva, Switzerland, p. 151 (2014)
26. Jevrejeva, S., Moore, J.C., Grinsted, A., Woodworth, P.L.: Recent global sea level acceleration started over 200 years ago? Geophysical Research Letters **35**(8), n/a–n/a (2008). DOI 10.1029/2008GL033611
27. Jongman, B., Ward, P.J.J., Aerts, J.C.J.H.: Global exposure to river and coastal flooding: Long term trends and changes. Global Environmental Change **22**(4), 823–835 (2012). DOI https://doi.org/10.1016/j.gloenvcha.2012.07.004
28. Keller, C.F.: Global warming: a review of this mostly settled issue. Stochastic Environmental Research and Risk Assessment **23**(5), 643–676 (2009). DOI 10.1007/s00477-008-0253-3. URL https://doi.org/10.1007/s00477-008-0253-3
29. Levy, J.K., Hall, J.: Advances in flood risk management under uncertainty. Stochastic Environmental Research and Risk Assessment **19**(6), 375–377 (2005). DOI 10.1007/s00477-005-0005-6. URL https://doi.org/10.1007/s00477-005-0005-6
30. Lin, N., Shullman, E.: Dealing with hurricane surge flooding in a changing environment: part i. risk assessment considering storm climatology change, sea level rise, and coastal development. Stochastic Environmental Research and Risk Assessment **31**(9), 2379–2400 (2017). DOI 10.1007/s00477-016-1377-5. URL https://doi.org/10.1007/s00477-016-1377-5
31. Meakin, P.: Fractals, Scaling and Growth Far from Equilibrium. Cambridge Nonlinear Science Series 5 (1998)
32. Milne, G.A., Gehrels, W.R., Hughes, C.W., Tamisiea, M.E.: Identifying the causes of sea-level change. Nature Geoscience **2**(7), 471–478 (2009). DOI 10.1038/ngeo544
33. Moftakhari, H.R., Salvadori, G., AghaKouchak, A., Sanders, B.F., Matthew, R.A.: Compounding effects of sea level rise and fluvial flooding. Proceedings of the National Academy of Sciences **114**(37), 9785–9790 (2017)
34. Mörner, N.A.: Some problems in the reconstruction of mean sea level and its changes with time. Quaternary International **221**(1), 3–8 (2010). DOI https://doi.org/10.1016/j.quaint.2009.10.044
35. Oliphant, E.J.E.T., Peterson, P., et al.: SciPy: Open source scientific tools for Python. URL http://www.scipy.org/
36. Permanent Service for Mean Sea Level (PSMSL): Tide Gauge Data. Retrieved Oct 2017 from http://www.psmsl.org/data/obtaining/ (2017)
37. Pugh, D.: Changing Sea Levels: Effects of Tides, Weather and Climate. Cambridge University Press, Cambridge, United Kingdom and New York, NY, USA (2004)
38. Pugh, D.T.: Tides, surges and mean sea-level (reprinted with corrections). John Wiley & Sons, Chichester, UK (1996)
39. Python Software Foundation: Python Language Reference, version 2.7. URL https://www.python.org/
40. Rahmstorf, S., Vermeer, M.: Discussion of: Houston, J.R. and Dean, R.G., 2011. Sea-Level Acceleration Based on U.S. Tide Gauges and Extensions of Previous Global-Gauge Analyses. Journal of Coastal Research, 27(3), 409–417. Journal of Coastal Research pp. 784–787 (2011). DOI 10.2112/JCOASTRES-D-11-00082.1
41. Severino, G.: Stochastic analysis of welltype flows in randomly heterogeneous porous formations. Water Resources Research **47**(3) (2011). DOI 10.1029/2010WR009840
42. Severino, G., Comegna, A., Coppola, A., Sommella, A., Santini, A.: Stochastic analysis of a field-scale unsaturated transport experiment. Advances in Water Resources **33**, 1188 – 1198 (2010)

43. Severino, G., De Bartolo, S., Toraldo, G., Srinivasan, G., Viswanathan, H.: Travel time approach to kinetically sorbing solute by diverging radial flows through heterogeneous porous formations. Water Resources Research **48**(12) (2012). DOI 10.1029/2012WR012608
44. Severino, G., Monetti, V., Santini, A., Toraldo, G.: Unsaturated transport with linear kinetic sorption under unsteady vertical flows. Transport in Porous Media **63**, 147 – 174 (2006)
45. Severino, G., Santini, A., Sommella, A.: Macrodispersion by diverging radial flows in randomly heterogeneous porous media,. Journal of Contaminant Hydrology **123**, 40 – 49 (2011)
46. Sivakumar, B.: Global climate change and its impacts on water resources planning and management: assessment and challenges. Stochastic Environmental Research and Risk Assessment **25**(4), 583–600 (2011). DOI 10.1007/s00477-010-0423-y. URL https://doi.org/10.1007/s00477-010-0423-y
47. Sornette, D.: Critical phenomena in natural sciences. Springer-Verlag Berlin Heidelberg, Germany (2000)
48. Tal, E., Atkinson, L.P., Corlett, W.B., and Blanco, J.L.: Gulf stream's induced sea level rise and variability along the U.S. midatlantic coast. Journal of Geophysical Research: Oceans **118**(2), 685–697 (2013). DOI 10.1002/jgrc.20091
49. Thorarinsdottir, T.L., Guttorp, P., Drews, M., Kaspersen, P.S., de Bruin, K.: Sea level adaptation decisions under uncertainty. Water Resources Research **53** (2017). DOI 10.1002/2016WR020354
50. Tomasicchio, G.R., Sánchez-Arcilla, A., D'Alessandro, F., Ilic, S., James, M.R., Sancho, F., Fortes, C.J., Schüttrumpf, H.: Large-scale experiments on dune erosion processes. Journal of Hydraulic Research **49**(sup1), 20–30 (2011). DOI 10.1080/00221686.2011.604574
51. Visser, H., Dangendorf, S., Petersen, A.C.: A review of trend models applied to sea level data with reference to the "acceleration-deceleration debate". Journal of Geophysical Research: Oceans **120**(6), 3873–3895 (2015). DOI 10.1002/2015JC010716
52. van der Walt, S., Colbert, S.C., Varoquaux, G.: The numpy array: A structure for efficient numerical computation. Computing in Science & Engineering **13**(2), 22–30 (2011). DOI 10.1109/MCSE.2011.37
53. Watson, P.J.: Is There Evidence Yet of Acceleration in Mean Sea Level Rise around Mainland Australia? Journal of Coastal Research pp. 368–377 (2011). DOI 10.2112/JCOASTRES-D-10-00141.1
54. Woodworth, P.L.: A search for accelerations in records of European mean sea level. International Journal of Climatology **10**(2), 129–143 (1990). DOI 10.1002/joc.3370100203
55. Woodworth, P.L., Pugh, D.T., Meredith, M.P., Blackman, D.L.: Sea level changes at Port Stanley, Falkland Islands. Journal of Geophysical Research: Oceans **110**(C6), 2156–2202 (2005). DOI 10.1029/2004JC002648
56. Woodworth, P.L., White, N.J., Jevrejeva, S., Holgate, S.J., Church, J.A., Gehrels, W.R.: Evidence for the accelerations of sea level on multi-decade and century timescales. International Journal of Climatology **29**(6), 777–789 (2009). DOI 10.1002/joc.1771
57. Wöppelmann, G., Zerbini, S., Marcos, M.: Tide gauges and Geodesy: a secular synergy illustrated by three present-day case studies. Comptes rendus - Géoscience **338**(14), 980–991 (2006)
58. Wu, S., Feng, A., Gao, J., Chen, M., Li, Y., Wang, L.: Shortening the recurrence periods of extreme water levels under future sea-level rise. Stochastic Environmental Research and Risk Assessment **31**(10), 2573–2584 (2017). DOI 10.1007/s00477-016-1327-2. URL https://doi.org/10.1007/s00477-016-1327-2
59. Zhang, Y., Ge, E.: Temporal scaling behavior of sea-level change in Hong Kong - Multifractal temporally weighted detrended fluctuation analysis. Global and Planetary Change **100**, 362–370 (2013)